



This is a repository copy of *Observations of Film Thickness Profile and Cavitation Around a Journal Bearing Circumference*.

White Rose Research Online URL for this paper:
<http://eprints.whiterose.ac.uk/94787/>

Version: Accepted Version

Article:

Kasolang, S. and Dwyer-Joyce, R.S. (2008) Observations of Film Thickness Profile and Cavitation Around a Journal Bearing Circumference. *Tribology Transactions*, 51 (2). pp. 231-242. ISSN 1040-2004

<https://doi.org/10.1080/10402000801947717>

Reuse

Unless indicated otherwise, fulltext items are protected by copyright with all rights reserved. The copyright exception in section 29 of the Copyright, Designs and Patents Act 1988 allows the making of a single copy solely for the purpose of non-commercial research or private study within the limits of fair dealing. The publisher or other rights-holder may allow further reproduction and re-use of this version - refer to the White Rose Research Online record for this item. Where records identify the publisher as the copyright holder, users can verify any specific terms of use on the publisher's website.

Takedown

If you consider content in White Rose Research Online to be in breach of UK law, please notify us by emailing eprints@whiterose.ac.uk including the URL of the record and the reason for the withdrawal request.



eprints@whiterose.ac.uk
<https://eprints.whiterose.ac.uk/>

Observations of Film Thickness Profile and Cavitation around a Journal Bearing Circumference

S. Kasolang^{1,2} and R. S. Dwyer-Joyce¹

¹Department of Mechanical Engineering, University of Sheffield, Sheffield, UK

²Faculty of Mechanical Engineering, Universiti Teknologi MARA, Malaysia

Keywords

film thickness measurement; ultrasound; journal bearing; cavitation

Abstract

The film formation in a journal bearing and the extent of the cavitated region is an important contribution to load carrying capacity. In the present work, an ultrasonic method has been used to measure the film thickness profile around the circumference of an operating journal bearing. The reflection of an ultrasonic pulse at an oil layer can be used to determine the film thickness. A transducer was mounted inside a hollow shaft and the signal passed through slip rings. The journal bearing was run at a series of loads and rotational speeds. The transducer continuously pulsed and received as it swept around the bush circumference. This enabled the full film thickness profile to be established. In the converging region the predicted film shape agrees well with predictions from classical lubrication theory. When cavitation occurs, the presence of oil-air and aluminium-air interfaces disrupts the ultrasonic signal. The extent of the cavitated region is clearly observed in the measurements. The minimum film thickness, the attitude angle, and the onset of cavitation are compared with theoretical solutions.

Introduction

The formation of a hydrodynamic oil film in a rotating journal bearing is well understood. There are well established models to predict the bearing eccentricity ratio and minimum oil film thickness. For most engineering applications, this is sufficient design information. However, in some cases, an understanding of the behaviour around the full film profile is important. For high precision highly loaded bearing, the effect of cavitation in the bearing is of interest. Cavitation occurs when the dissolved gas comes out of solution as the pressure falls in the diverging section of the bearing. If the pressure drop is low enough then the lubricant itself may evaporate. This vaporous cavitation is particularly important because it can lead to surface pitting by bubble collapse.

Another significant aspect of the film profile is the presence of entrained air or vapour bubbles. Bubbly oil is believed to have increased load carrying capacity by enhancing the oil viscosity [1, 2]. Where the bearing is subject to dynamic squeeze action, the presence of bubbles is known to significantly affecting the load carrying capacity [3].

Progress in the study of bearing cavitation has been reviewed in several papers [4-6]. Reynolds' equation with a cavitation boundary condition is generally used to describe the lubricant flow. However under certain circumstances, description by Reynolds' equation is insufficient to describe the film rupture observed in the cavitation region. Consideration of other models such as

those proposed by Floberg [7-9] and Coyne and Elrod [10,11] is necessary to avoid significant errors. When the journal is lightly loaded, the eccentricity ratio determines the proper mathematical model to use. In general, Coyne and Elrod [10,11] prediction is suggested for higher eccentricity ratio and Floberg's model [7-9] for lower eccentricity ratio. Gropser and Etsion [12] compared the former model with experiments and found a close agreement for the location of the onset of cavitation. Their work also concluded that the cavitation shape is influenced by the shear of the cavity gas bubble.

The method for visualising film formation, based on a transparent bush and suitable lighting, has demonstrated how 'fingers' of air form in the convergent region [4]. This can be suppressed by the use of large lubricant supply grooves (or partial arc bearings) and a high pressure inlet. However the precise location of the cavitation front is difficult to control as it varies with eccentricity, supply pressure, and lubricant. For these reasons a method of measurement around the complete circumference and the detection of the cavitated zone would be useful.

In the present study, an approach based on the reflection of ultrasound was used to provide the complete film profile. The reflection of an ultrasonic pulse at the oil film was recorded as the transducer was swept around the film. This can be used to study not only the minimum film thickness but also the extent of the cavitated region.

Ultrasonic Measurement and Oil Film Thickness

The ultrasonic technique provides a suitable method for oil film thickness measurements without the need to make extensive modification to the bearing parts [14]. The concept is simple and robust. A wave of ultrasound striking on oil film will be partially transmitted and partially reflected. If the oil film is thin compared with the ultrasonic wavelength, then a simple quasi-static spring model can describe the response of the layer [15]. The magnitude of the reflection coefficient (the amplitude of the reflected wave divided by that of the incident wave) is given by:

$$|R| = \frac{\sqrt{(\omega z_1 z_2)^2 + K^2 (z_1 - z_2)^2}}{\sqrt{(\omega z_1 z_2)^2 + K^2 (z_1 + z_2)^2}} \quad (1)$$

where ω is the angular frequency of the incident wave and z_1 and z_2 is the acoustic impedance of the materials either side of the oil film. The acoustic impedance is the product of the density and the wave speed in the material. K is the stiffness of the oil film (expressed per unit area).

The stiffness of an oil film is a function of its bulk modulus, B and film thickness, h according to:

$$K = \frac{B}{h} \quad (2)$$

Or in terms of the oil's acoustic properties:

$$K = \frac{\rho c^2}{h} \quad (3)$$

where ρ is the oil density and c is the speed of sound in the oil. The film thickness can then be expressed in terms of reflection coefficient by combining (1) and (3):

$$h = \frac{\rho c^2}{\omega z_1 z_2} \sqrt{\frac{R^2 (z_1 + z_2)^2 - (z_1 - z_2)^2}{1 - R^2}} \quad (4)$$

Thus, if the properties of the oil and the media either side are known, then the reflection coefficient can be used to determine the oil film thickness.

The experimental application of the model has been validated in [14] and used to study film thickness in a journal bearing [16]. In the latter study, readings were recorded from the stationary bush at a single location corresponding to the maximum load point.

Measurement Apparatus

Journal bearing test apparatus

A schematic of the journal bearing test rig is shown in Fig. 1(a). A steel shaft was rotated by an electric motor through a belt drive. A brass bush was pressed into a loading frame. A hydraulic load was applied to the frame as shown. The journal had a single oil inlet (no lubricating grooves). Table 1 shows the dimensions of the test bearing. A mineral oil (Shell Turbo T68) was supplied at a slight positive pressure (1.5 to 2.0 bar) to ensure starvation did not occur during testing.

An ultrasonic transducer was assembled inside the shaft of a journal bearing (details follow in the next section) as shown in Fig. 1(b). Oil temperature was recorded using thermocouples at the oil inlet and outlet of the bearing. The bearing load and speed were monitored throughout using a simple load cell and laser tachometer.

Ultrasonic measurement equipment

The components of the ultrasonic system used were the PC, transducer, ultrasonic pulser receiver (UPR), and oscilloscope. A schematic diagram of the apparatus is shown in Fig. 2. The PC was used to control the UPR, which supplied short-period top hat voltage pulses to the transducer. The piezo-electric transducer causes a displacement pulse under an applied voltage. The transducer is arranged so the pulse is emitted normal to the oil film (the curvature of the journal has only a minor effect).

The pulse is partially reflected and is recorded by the same transducer. The signal is amplified by the UPR, then digitised by the oscilloscope and downloaded to the PC for further analysis and display. A Labview interface was written to control the UPR, capture signals, and digital processing.

Transducer Installation

The ultrasonic transducer used was a piezoelectric disk of thickness 2 mm and diameter 10 mm as shown in Fig. 3(a). The nominal frequency is 1 MHz. The resulting centre frequency was 1.2 MHz. The transducer was bonded to an aluminium plug using high temperature cyanoacrylate glue. The plug was then pres-fitted into a machined hole in the journal and the outer bore ground to size.

Aluminium was chosen for the plug material. This is because it has similar acoustic impedance to brass and so in equation (4) the $(z_1 - z_2)$ term is small. This means that there is a wide reflection coefficient range to work with and so will increase the film thickness range that can be accurately measured by the transducer.

One contact was soldered to the top face of the transducer and the second to the aluminium plug (as shown in Fig. 3(b)). The contacts wires were then soldered to anchor pads and then the main

wires fed back through slip rings to the pulsing-receiving circuit. The piezo and soldered contacts were then covered in a protective layer of epoxy.

Signal processing

In order to obtain the reflection coefficient needed for equation (4) it is required to obtain both reflected and incident signals. The simplest way to determine the incident signal was to record a reflection when there was no oil at the interface (journal and sleeve disengaged). In this case the pulse was virtually fully reflected and so the incident signal equalled the reflected signal. All subsequent signals from oil films were divided by the reference signal to obtain the reflection coefficient. Signals were recorded in time domain and later transformed into frequency domain using the Fast Fourier Transform (FFT) to obtain amplitude spectra.

Inspection of Fig. (4) shows that the reflection coefficient will depend on the frequency of the wave. The full amplitude spectrum was recorded and equation (4) used to obtain the film thickness at all frequencies. The film thickness is independent of frequency so the result is a straight line. In practice, it is not necessary to record the full waveform but instead calculations are performed using just the centre frequency of the transducer where energy is maximum.

The reflection coefficient recorded from the oil layer was plotted against the angular position around the journal. Sufficient data were required to get a good film thickness profile per revolution. The rate of digitisation and transfer of data from the scope to the PC was too slow to achieve this if the full reflection was to be recorded. Instead only the required reflection data segment at the aluminium-oil-brass interface was stored on the scope's internal memory. The scope had the memory to store 500 segments. The sampling rate was 50 Ms.s^{-1} and each segment contains 250 points. This corresponds to approximately 210 data points per revolution of 300 rpm (or 1 point for every 1.7°). These data were later transferred in one block for post-processing.

Results and Discussion

Static Measurement of Journal Bearing Clearance

A series of preliminary tests were carried out to measure the bearing cavity when static. This was to ensure accuracy of the readings and that the concentricity and dimensions of the journal were correct. The bearing cavity was flooded with oil and a very low load was applied. The shaft was then rotated by hand and the reflected signal was recorded at several different locations. The reflection coefficient was correlated to film thickness using equation (1).

The resulting film thickness profile is shown in Fig. 4. The geometrical predicted profile of the gap is also shown (for the case when the radial clearance is $25 \mu\text{m}$).

A slight bump in the film thickness profile in the converging region (between $120^\circ < \theta < 180^\circ$) was observed. The bump implies that the calculated film thickness is larger than the predicted values. This was due to slight out of roughness of the bush. Later plots (Figs 7 and 8) of film thickness measurements also show a slight anomalous bump in this region caused by the superposition of the geometric irregularity. As the gap thickness approaches $50 \mu\text{m}$ the scatter in the results increases. This is because the reflection coefficient is approaching unity and then, by inspection of equation (4), a small variation due to noise causes a large variation in the film thickness calculated. To optimise the measurements a low frequency transducer could be used to measure these thicker films. The reflection coefficient would then be lower, however too low a frequency will not permit the measurement of the thinnest films as the reflection tends to zero.

Temperature Compensation for Measured Reflection Coefficient

Measurement of film thickness is based on the variation in the amplitude of the reflected ultrasonic pulse from an oil layer divided by a measured reflection when no oil is present (the reference pulse). The energy output from piezo-electric materials is subject to variation with temperature. In addition the adhesive attenuation can also change with temperature. If this occurs during a test the reflection coefficient will change, as the reference trace was recorded in the cold state.

Frictional heating will cause the temperature of the journal to rise due to over time. The piezo output will also change. This becomes especially critical as the reflection coefficient approaches unity when the film thickness is large. As described above, in this region a small variation in R can cause a big variation in the calculated film thickness.

To compensate for this thermal drift, the reflected reference pulse was recorded after a test when the journal was disengaged but still warm. A thermocouple was placed right on the outer surface of the aluminium plug onto which the piezo sensor was attached. The variation in surface temperature and the reflected pulse was recorded as the journal cooled down. The results are shown in Fig. 5. A linear curve fit produces a mathematical equation that can be used for the thermal correction factor.

Variation in Reflection Coefficient Data

Fig. 6 illustrates the journal bearing geometry with fluid layer formed by clockwise rotation. The thickness of the fluid layer varies around the journal, which can be determined from bearing geometry. The co-ordinate θ has its origin at the line passing through the bush and journal centres; the attitude angle ϕ is measured from that line to the vertical.

For this bearing, the bush can be assumed to be rigid so the film thickness profile should be symmetrical over the line passing through the maximum, h_{max} (0°) and the minimum, h_{min} (180°) locations. The region where the fluid converges (below the symmetrical line) is known as the film formation region. Conversely, the region where the fluid diverges is called the film rupture region.

Fig. 7 shows a series of reflection coefficient profiles recorded around the circumference for increasing bearing load. Each set of data shows a distinct reflection coefficient minimum corresponding to the minimum film thickness (this data point was set at an angular position of 180°). In the converging section (0° to 180°) the reflection reduces as the oil film reduces in the wedge. At higher load, this reduction is greater, corresponding to the steeper wedge formed by a more eccentric journal.

The distribution is clearly not symmetrical about $\theta=180^\circ$. Immediately after the minimum point, there is a sudden increase in R as cavitation occurs. The lower load cases show only a slight increase, as the condition is less severe. In the divergent part, the gap is filled with a mixture of oil and suspended air. This has three possible effects on ultrasonic reflection. Firstly a large aluminium-air or oil-air interface will completely reflect any incident ultrasound (R tends to one). Secondly, a distribution of large air bubbles will act to scatter the sound waves, R will be reduced. And thirdly, smaller suspended air bubbles will cause the effective density and wave speed in the oil to reduce. In each case the oil film thickness will be over-predicted because of the apparent signal loss due to attenuation or scatter.

As mentioned above, as R tends to unity, equation (4) shows that h tends to infinity and small errors in R lead to big errors in h. The resulting error will depend on the noise in the reflected signals, which in turn depends on the quality of the electronic equipment and electromagnetic shielding. Past experience [16] suggests that data in the region $R<0.95$ gives satisfactory measurements of h. This limit is plotted on the graph.

Conversion to Film Thickness

The data for three of the load cases from Fig. 7 has been converted to film thickness using equation (4). The calculation is strictly only valid in the converging section of the bearing. The results are shown in Fig. 8 (a) to (e) for five different loads. The data shown in grey represent the cases where $R>0.95$ and the model becomes unstable.

The predicted minimum film thickness is also shown on the plot. The film thickness is given by:

$$h = c(1 + \varepsilon \cos \theta) \quad (5)$$

where c is the radial clearance and θ is the angular position measured from the maximum film thickness location. The corresponding eccentricity ratio, ε was obtained using the method described in [17] based on the hydrodynamic solutions of Raimondi and Boyd [18]. This solution is isothermal. The temperature of the lubricant increases by $\sim 20^\circ$ from the inlet to the outlet; this will change its viscosity. Two predictions are plotted on Fig. 10; one assuming the oil remains at the inlet temperature and one assuming it is at the outlet temperature throughout.

Over the converging section $120^\circ < \theta < 180^\circ$ the agreement between the measured film and the hydrodynamic prediction is close. As soon as cavitation occurs the predicted film rises rapidly. It is possible that the capture is not fast enough to record some data points where the signal may have reached $R=1$. In the diverging part, where the data deviate from the theoretical line, air bubbles have formed. At around $\theta=220^\circ$ the air is being dispersed and the film starts to reform. The predicted film is still higher than it should be because the oil contains dispersed air bubbles. For the highest load case the reflection dips immediately after the cavitation region and then rises again. The reasons for this are not clear, possibly smaller bubbles are coalescing and acting as ultrasonic scatterers. At $\theta=300^\circ$ - 320° fresh oil is pumped into the bearing cavity. This oil is free from second phase air and so the measured film thickness is close to the predicted value. In some cases it has dipped slightly below the predicted value. This is caused by the slight uncertainty in the temperature of the oil at this point. If it is lower than the value used for the prediction, the resulting film thickness will be lower.

Attitude Angle and Minimum Film Thickness

The measurement of the minimum film thickness and its location (attitude angle, ϕ) have been compared with the theoretical hydrodynamic solution [17]. The film thickness ratio is plotted against the Sommerfeld number:

$$S = \eta\omega \frac{LD}{W} \left(\frac{R}{c}\right)^2 \quad (6)$$

The attitude angle is obtained by comparing the positions of the oil film minimum to the oil inlet point. Fig. 9 and 10 show the results. There is a good agreement in both cases.

Location of the Onset of Cavitation

Hydrodynamic predictions (using the method of [17]) suggest that the onset of cavitation varies from 198° for the 3 kN case to 195° for the 10 kN case. From the plots of Fig. 10, it is not immediately obvious at which location cavitation first starts to occur. There is no sharp boundary between a measurable reflection coefficient and one that tends to unity. There is possibly a spacing of a few degrees past the minimum film thickness point where the measured film still agrees with the predicted one. However the transition to a peak in reflection is gradual. This suggests air bubbles are forming gently and there is not a sudden rupture of the film at the loads and speeds tested here.

Discussion

A key advance in this work has been the location of an ultrasonic transducer inside a rotating shaft. The signal has been passed through slip rings. Despite the high frequency nature of the signal transmitted, there have been no significant problems with and increase in signal noise. This has allowed the measurement of the film profile around the bearing circumference, rather than being restricted to one location. However, for this kind of study it is important to ensure the correct frequency of transducer is used. Each transducer has a limited bandwidth. The reflection coefficient should typically remain within the limits $0.05 < R < 0.95$ so that any noise present in the signal does not unduly affect the conversion to film thickness. The transducers used in this study had a bandwidth in the range 0.6 to 1.8 MHz. This meant that they were suitable for measuring films in the range 1 to $116 \mu\text{m}$. For the present bearing, of radial clearance $25 \mu\text{m}$, these transducers are adequate. The danger of using transducer in a rotating shaft where they are required to measure both thick and thin films is that their range must be such that this can be achieved (or more than one transducer must be used).

A further complexity is that the oil film temperature varies around the circumference of the bearing. This has two effects; the acoustic properties of the oil change (by about 0.2% per $^\circ\text{C}$), and the transducer output varies (by about 0.5% per $^\circ\text{C}$). It is possible to compensate for the latter; this is easily done using some kind of calibration curve (as shown in Fig. 4). The temperature at the sensor needs to be measured. It is not so easy to compensate for the former since it varies around the circumference and would require measurement of the film temperature at a number of locations. In this work a mean film temperature has been used as the variation is not great.

The measurement of an oil film ultrasonically relies on the liquid being homogeneous of known acoustic properties (density and speed of sound). In the inlet region these conditions are fulfilled

and the measured oil film thickness agrees with predictions based on classical hydrodynamic theory. Both the attitude angle and minimum film thickness measurements are reliable.

In the diverging part of the bearing cavitation occurs and the presence of macro pockets of air or distributed air bubbles modify the reflected signal. This happens by the large pockets of air fully reflecting the ultrasonic wave, and small suspensions causing a reduction in the speed of sound. For small quantities of finely dispersed second phase, the speed of sound in a two phase mixture, c can be described the so-called Urlick [19] equation:

$$c = \frac{1}{\sqrt{\left(\frac{\phi}{\rho_a c_a^2} + \frac{(1-\phi)}{\rho_o c_o^2}\right)(\phi \rho_a + (1-\phi)\rho_o)}} \quad (7)$$

where ϕ is the air volume fraction, ρ is the density, c the speed of sound, and the subscripts a and o stand for air and oil respectively. A small fraction of air can have a significant effect on the speed of sound. Oil typically contains about 8% of dissolved air. This is easily enough to upset the acoustic measurements should full cavitation takes place. The reflection coefficient then tends to unity and the calculated oil film tends to infinity.

The proportion of the second phase suspended air varies around the journal. Thus the speed of sound will also change. In the inlet zone there are no suspended bubbles. In the diverging zone $220^\circ < \theta < 300^\circ$, the required speed of sound to make the results ‘fit’ the model is between 500 and 1300 m/s. This corresponds to around 0.1 – 0.01% suspended air. However, the effect of this second phase on the reflection of ultrasound is complex and there is little merit in trying to draw too many conclusions as to the nature of the film from the reflected signal. The transducer is probably best used to detect the onset of cavitation rather than any detailed predictions about what is happening inside the cavitated region.

In a stiff bearing of the kind used here the location of the cavitation region is well defined. But in an elastically deforming bearing shell, this is not the case. The deformation is a function of the film pressure distribution that in turn depends on the extent of the cavitation region. Ultrasonic measurements around the circumference could prove useful in bearings of this kind.

Conclusions

A journal bearing test rig has been built with an ultrasonic sensor located inside a hollow shaft. It has proved possible to transit the high frequency ultrasonic signal through a conventional set of slip-rings.

The reflection of an ultrasonic pulse is related to the stiffness of the oil film and hence the oil film thickness. The film thickness profile has been recorded around the bearing circumference under a range of loads and speeds. The profile obtained in the converging region agrees well with classical hydrodynamic predictions. The minimum film thickness and attitude angle measurements also agree well.

However, as soon as cavitation occurs the presence of second phase air provides another source of attenuation or reflection of ultrasound. This means that the conversion from reflection coefficient to oil film thickness is no longer valid.

Whilst quantitative film measurements are no longer possible in the diverging zone, the form of the data reveals information about the onset of cavitation and reformation of the film. The results

indicate an arc of around 20-30° over which severe cavitation occurs followed by expulsion or re-absorption of the air.

Provided the effects of cavitation can be separated from genuine film thickness measurements, this approach can be useful in film thickness determination in elastically deforming bearings, or to study the effect of oil grooves.

References

- [1] Tonder, K. (1975), "Effect of Bubbly Lubricant on Bearing Performance," in Proc. of JSLE/ASLE Conference.
- [2] Nikolajsen, J.L. (1999), "Viscosity and Density Models for Aerated Oil in Fluid-Film Bearings," Trib. Trans., **42**, 1, pp186-191.
- [3] Cole, J.A., and C.J. Hughes (1957), "Visual study of film extent in dynamically loaded complete journal bearings," in Lubrication and Wear conf., Proc. Inst. Mech. Engrs., pp 147-149.
- [4] Dowson, D., and Taylor, C.M. (1979), "Cavitation in Bearings," A Rev. Fluid Mech., pp 35-66.
- [5] Heshmat, H. (1988), "Experimental Studies in Cavitation: Current Research in Cavitation Fluid Films," STLE Special Publications, SP-28, pp 4-8.
- [6] Brewster, D.E., and Khonsari, M. (1990), "Current Research in Cavitating Fluid Films: Part I. Fundamental and Experimental Observation" and "Part II: Theoretical Modelling," STLE Special Publication on Cavitation, SP-28.
- [7] Floberg, L. (1965), "On hydrodynamic lubrication on special with special reference to sub-cavity pressures and number of streamers in cavitation regions," Acta Polytech Scand. Mech. Eng. Ser., ME 19
- [8] Floberg, L. (1968), "Sub-cavity pressures and number of oil streamers in cavitation regions with special reference to the infinite journal bearing," Acta Polytech Scand. Mech. Eng. Ser., ME 37
- [9] Floberg, L. (1972), "Lubrication of two rotating cylinders at variable lubricant supply with special reference to the tensile strength of the liquid lubricant," ASME-ASLE Conf. New York, Pap. 72-Lub 2
- [10] Coyne, J.C., and Elrod, H.G. (1970), "Conditions for the rupture of a lubricating film, Part I: Theoretical Model," J. Lubr. Technol. Trans. ASME 92, pp 451-56
- [11] Coyne, J.C., and Elrod, H.G. (1971), "Conditions for the rupture of a lubricating film, Part II: New boundary conditions for Reynolds' equation," J. Lubr. Technol. Trans. ASME 93, pp 156-67
- [12] Groper, M and Etsion, I. (2001), "The effect of shear flow and dissolved gas diffusion on the cavitation in a submerged journal bearing," ASME Trans., Vol. 123, pp. 494-500
- [14] Dwyer-Joyce, R.S., Drinkwater, B.W., and Donohoe, C.J., (2002), "The Measurement of Lubricant Film Thickness using Ultrasound," Proceedings of the Royal Society Series A, Vol. 459, pp 957-976.
- [15] Reddyhoff, T., Kasolang, S., Dwyer-Joyce, R.S., and Drinkwater, B.W. (2005), "The phase shift of an ultrasonic pulse at an oil layer and determination of film thickness," Proc. Inst. Mech. Engrs., Part J 219, pp 387-400.

- [16] Dwyer-Joyce, R.S., Harper, P., and Drinkwater, B. (2004), "A Method for the Measurement of Hydrodynamic Oil Films Using Ultrasonic Reflection," *Tribology Letters*, Vol. 17, pp. 337-348.
- [17] Khonsari and Booser (2001), *Applied Tribology: Bearing Design and Lubrication*, John Wiley and Sons, Inc., New York.
- [18] Raimondi, A.A. and Boyd, J., (1958), "A solution for the finite journal bearing and its application to analysis and design -I -II, -III", *ASLE Trans.*, Vol. 1, No. 1, I- pp. 159-174, II - pp. 175-193, III - pp. 194-209.
- [19] Urick, R. J. (1947), "A sound velocity method for determining the compressibility of finely divided substances," *Journal of Applied Physics* 18, pp 983-987.

Diameter	75 mm
Length	37.5 mm
Radial clearance	25 μm
Load range,	2 – 10 kN
Speed range	200 – 800 rpm
Lubricant viscosity	46 cSt @ 40°C 8.8 cSt @ 100°C

Table 1: Dimensions of the test bearing, lubricant properties, and operating parameters.

List of Figures

Figure 1 (a) Schematic of the journal bearing test assembly, (b) Photograph and schematic of the journal and transducer.

Figure 2: Schematic diagram of the apparatus used for generating and receiving ultrasonic pulses.

Figure 3: (a) Piezo-electric disk and (b) schematic of assembly to plug.

Figure 4: Measured static bearing gap compared with the geometrical solution.

Figure 5: Variation in the ultrasonic reflection coefficient as the sensor temperature changes.

Figure 6: Schematic of Film Thickness Profile in Journal Bearing

Figure 7: Reflection coefficient measurements around the bearing circumference.

Figure 8: Measured film thickness profile for five bearing loads (a) 3 kN, (b) 6 kN, and (c) 10 kN, all rotating at 300 rpm. Theoretical solutions [17] are plotted for the case where the oil temperature is equal to the inlet temperature and the outlet temperature throughout.

Figure 9: Experimental and Predicted Minimum Film Thickness Ratio

Figure 10: Experimental and Predicted Attitude Angle

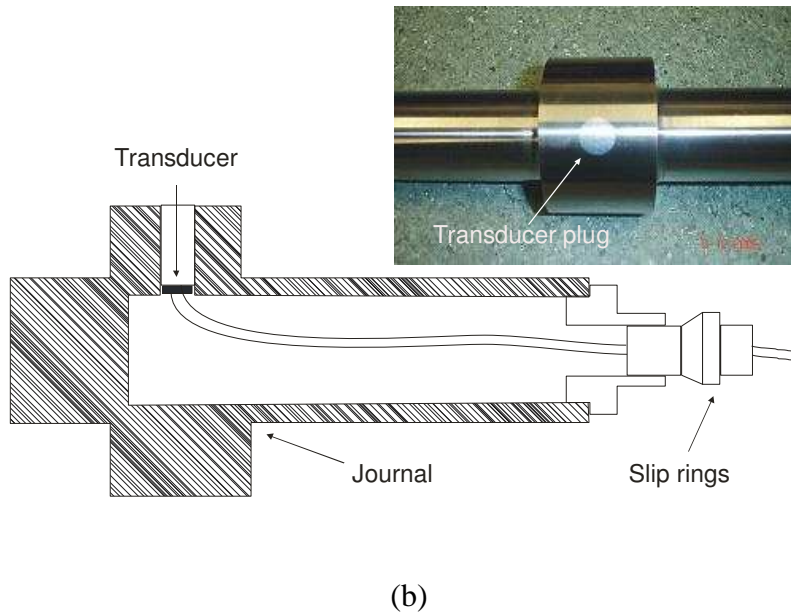
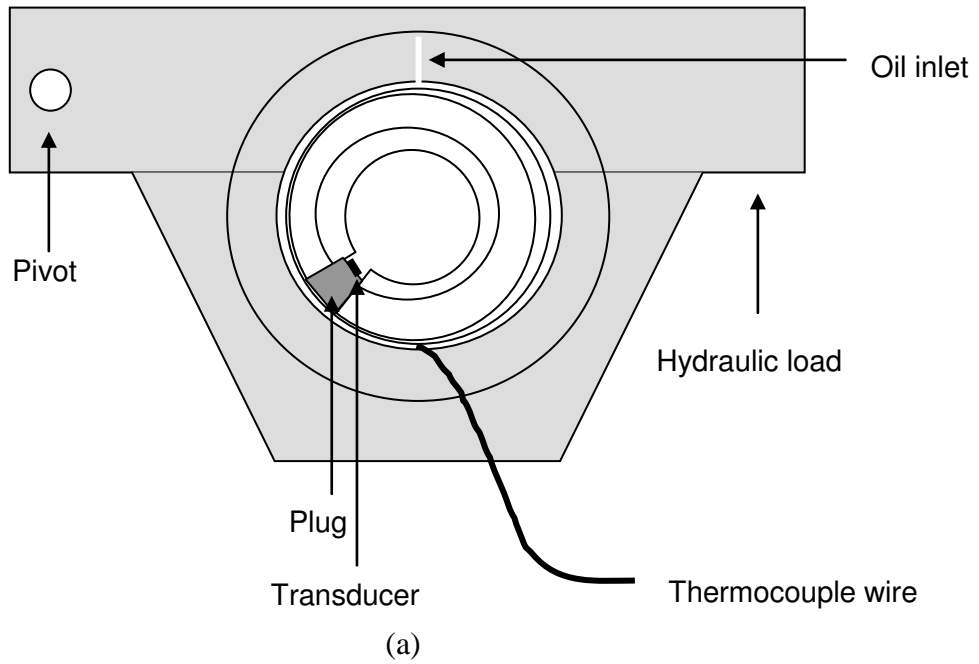


Figure 1 (a) Schematic of the journal bearing test assembly, (b) Photograph and schematic of the journal and transducer.

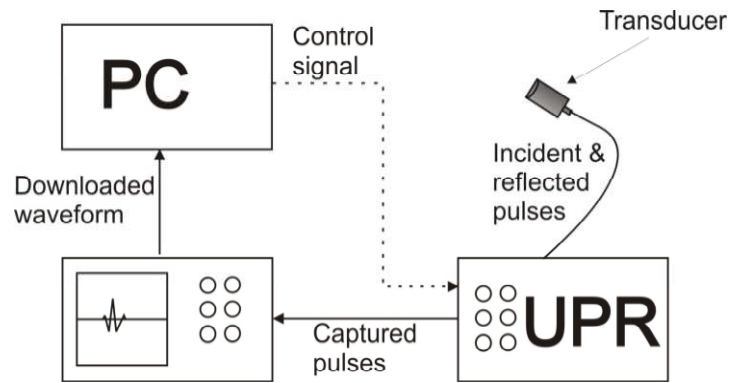
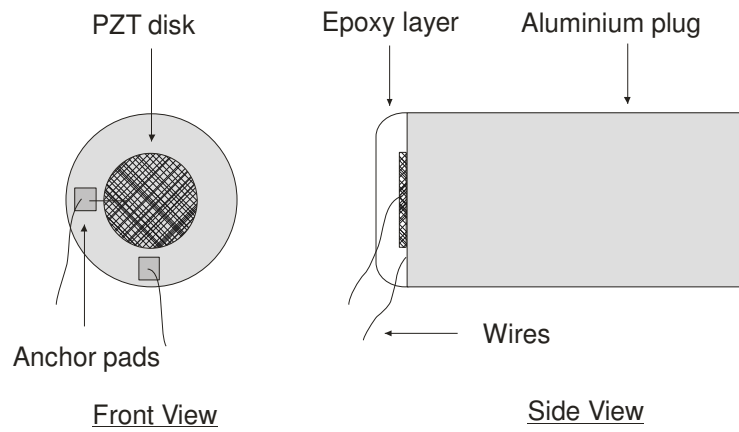


Figure 2: Schematic diagram of the apparatus used for generating and receiving ultrasonic pulses.



(a)



(b)

Figure 3: (a) Piezo-electric disk and (b) schematic of assembly to plug.

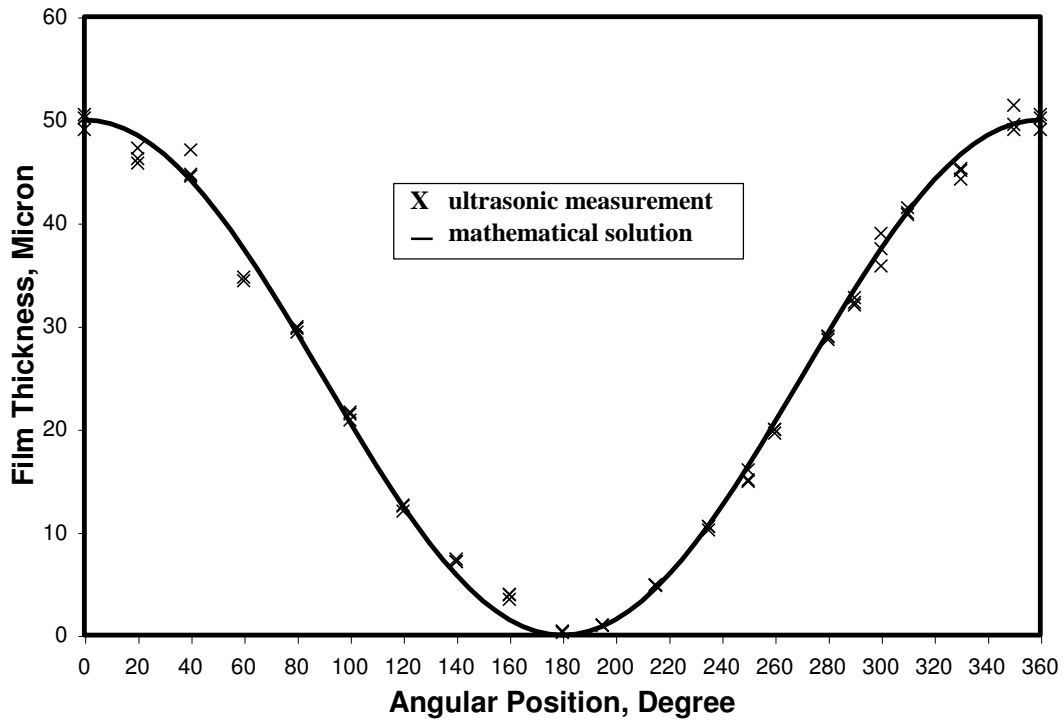


Figure 4: Measured static bearing gap compared with the geometrical solution.

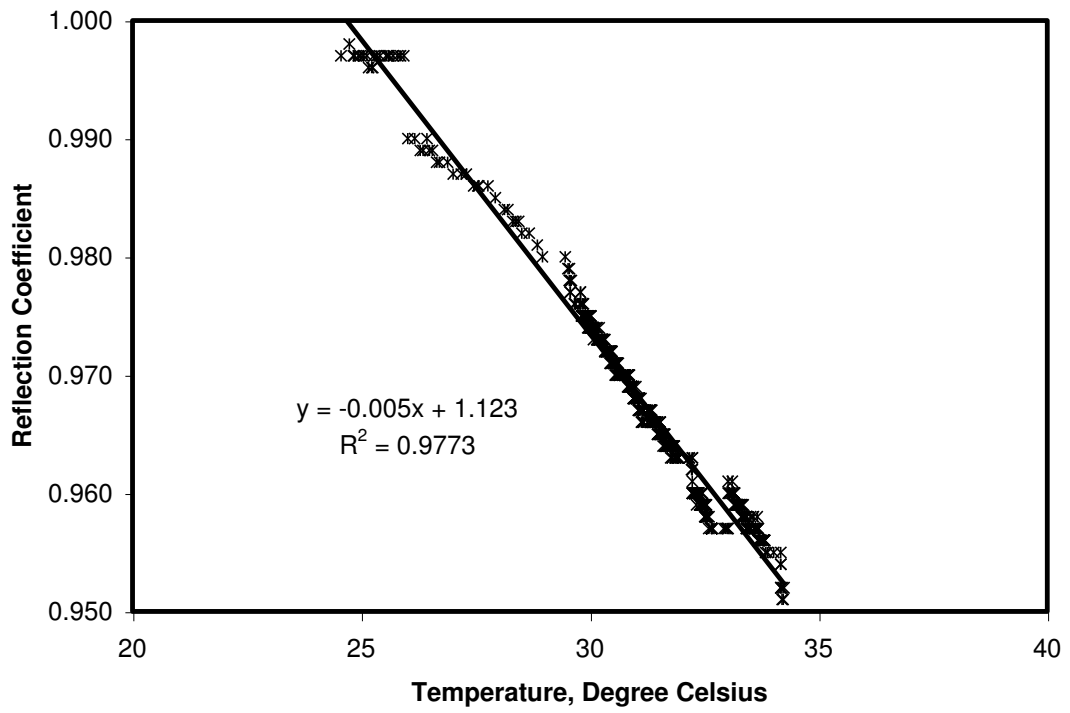


Figure 5: Variation in the ultrasonic reflection coefficient as the sensor temperature changes.

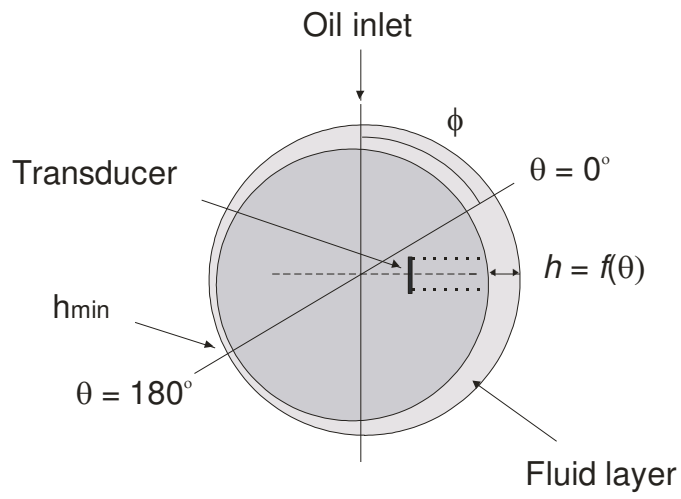


Figure 6: Schematic of Film Thickness Profile in Journal Bearing

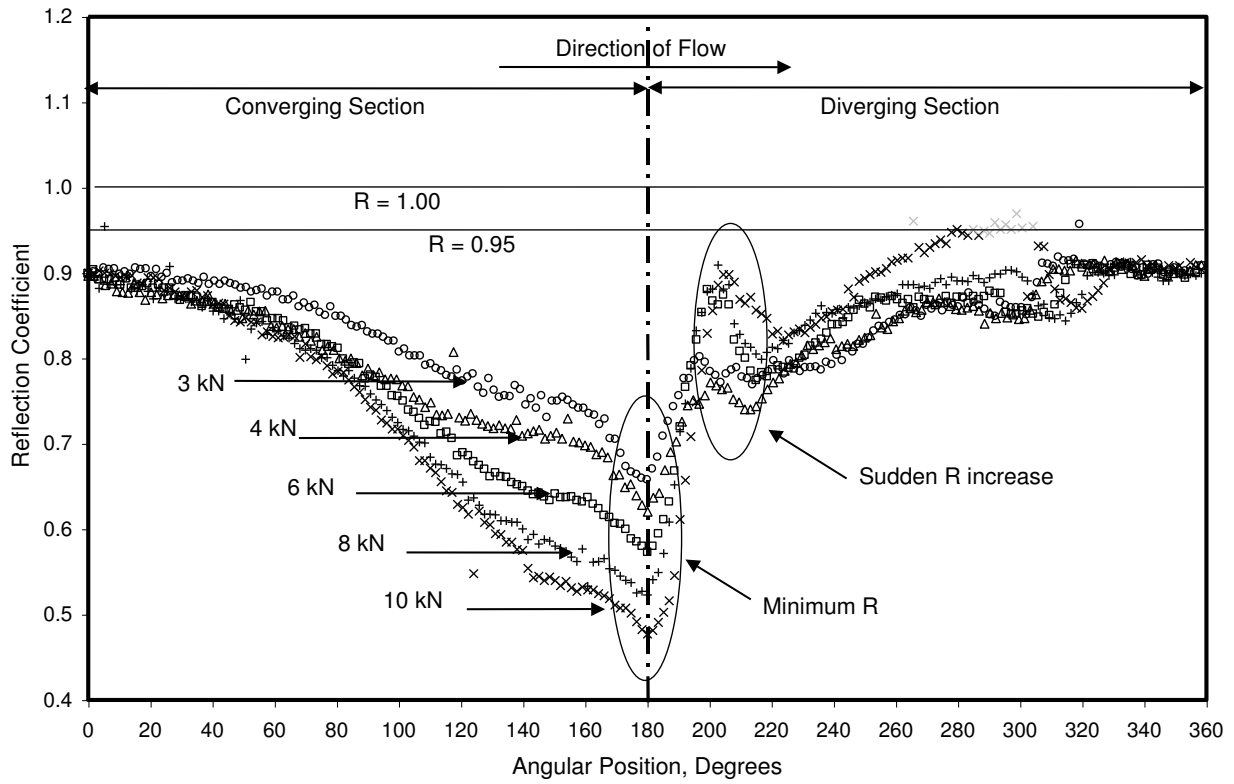
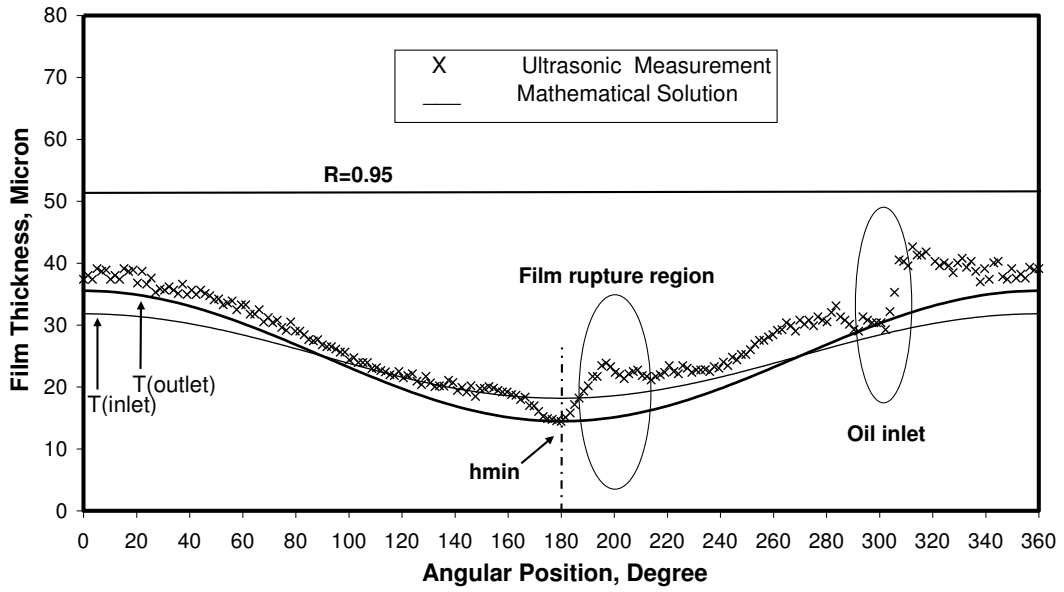
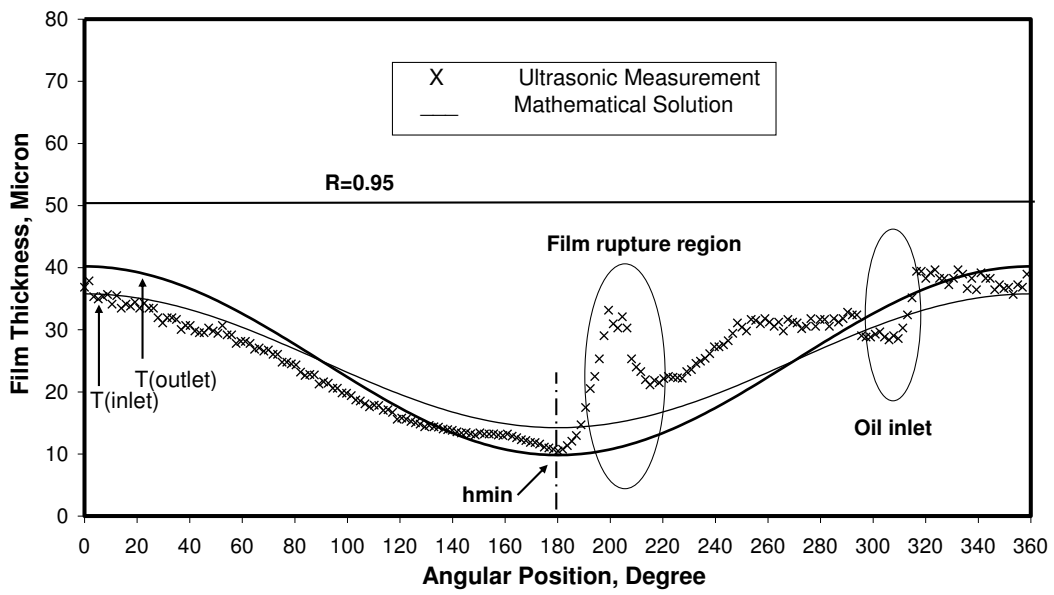


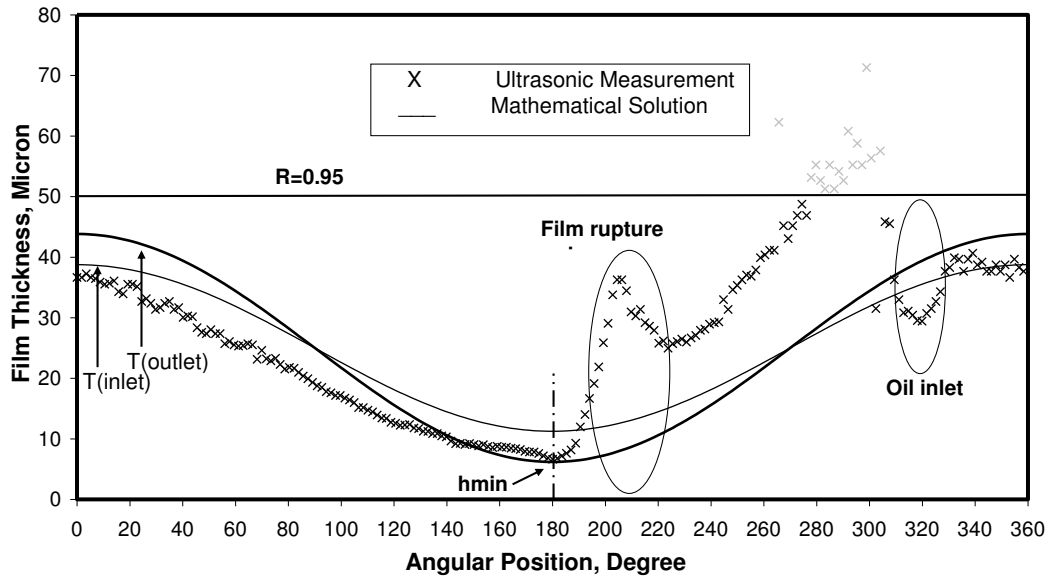
Figure 7: Reflection coefficient measurements around the bearing circumference.



(a)



(b)



(c)

Figure 8: Measured film thickness profile for five bearing loads (a) 3 kN, (b) 6 kN, and (c) 10 kN, all rotating at 300 rpm. Theoretical solutions [17] are plotted for the case where the oil temperature is equal to the inlet temperature and the outlet temperature throughout.

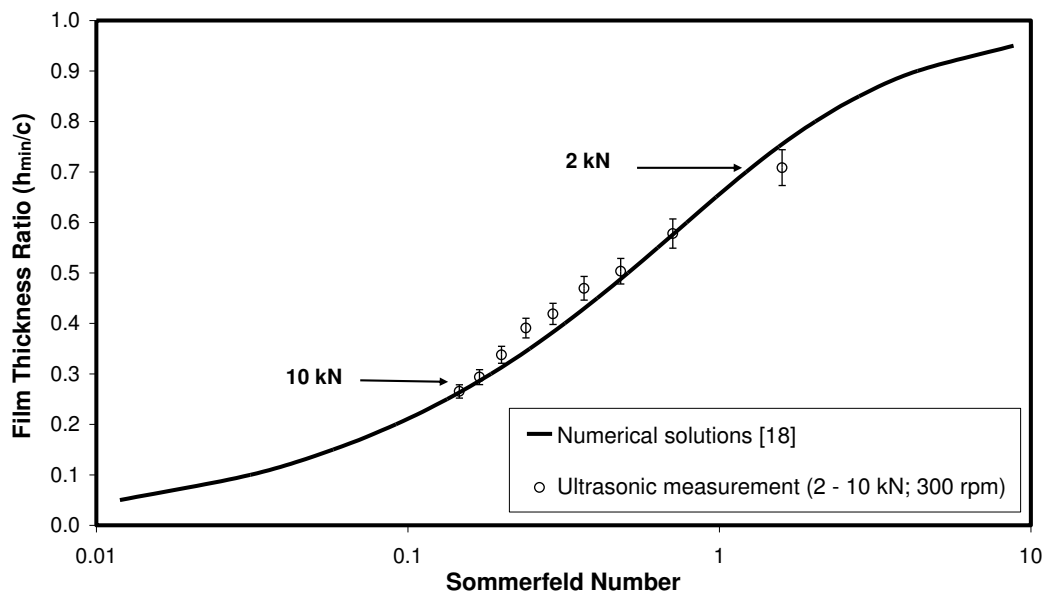


Figure 9: Experimental and Predicted Minimum Film Thickness Ratio

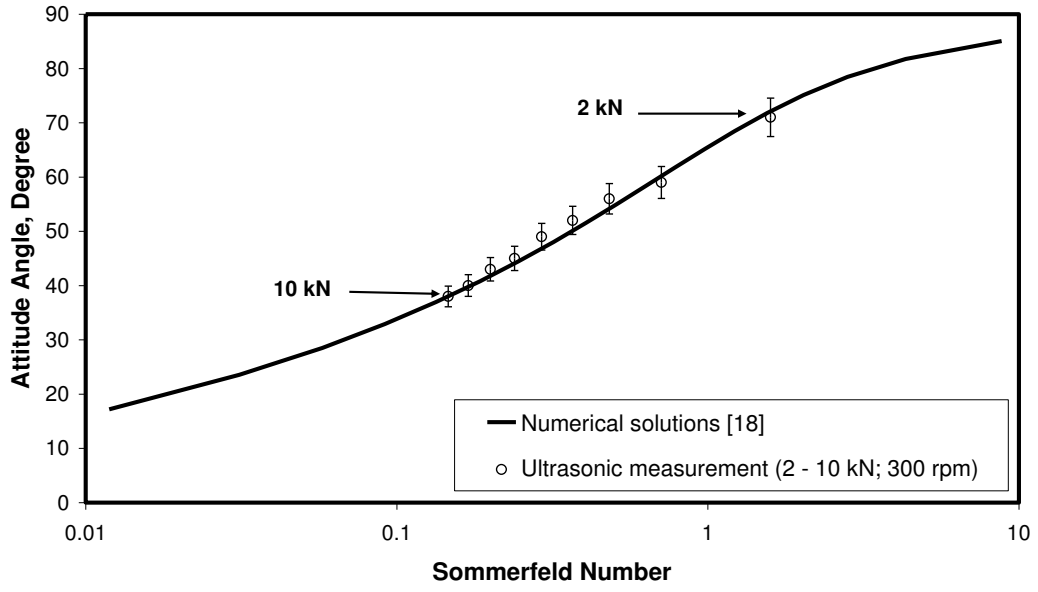


Figure 10: Experimental and Predicted Attitude Angle